ARTICLES
https://doi.org/10.1038/s43016-021-00230-y
nature food

Structure–function studies of chickpea and durum wheat uncover mechanisms by which cell wall properties influence starch bioaccessibility

Cathrina H. Edwards[1,4]✉, Peter Ryden[2], Giuseppina Mandalari[2,3], Peter J. Butterworth[1] and Peter R. Ellis[1]✉

Positive health effects of dietary fibre have been established; however, the underpinning mechanisms are not well understood. Plant cell walls are the predominant source of fibre in the diet. They encapsulate intracellular starch and delay digestive enzyme ingress, but food processing can disrupt their structure. Here, we compare the digestion kinetics of chickpea (cotyledon) and durum wheat (endosperm), which have contrasting cell wall structures (type I and II, respectively), to investigate a cell wall barrier mechanism that may underpin the health effects of dietary fibre. Using in vitro models, including the dynamic gastric model, to simulate human digestion, together with microscopy, we show that starch bioaccessibility is limited from intact plant cells and that processing treatments can have different effects on cell integrity and digestion kinetics when applied to tissues with contrasting cell wall properties. This new understanding of dietary fibre structure is important for effective fibre supplementation to benefit human health.

The long-term health benefits of dietary fibre include risk reduction and improved management of cardiometabolic diseases[1], yet the physiological mechanisms underpinning them are not fully understood. Terminology describing fibre in health relates to its solubility and/or composition, but the structure and properties of fibre as cell wall bioassemblies that encapsulate macronutrients have received much less attention[2]. Here, we consider mechanisms by which fibre influences starch bioaccessibility by comparing two widely consumed starch-staple crops with contrasting cell wall structures: chickpea (*Cicer arietinum* L.) and durum wheat (*Triticum durum* L.). Chickpeas, beans and other dicotyledonous plant seeds have type I primary cell walls that are rich in pectic polysaccharides and xyloglucans, whereas wheat and other monocotyledonous cereal grains have type II primary cell walls that are low in pectin but rich in arabinoxylans and/or mixed-linkage (1→3),(1→4)-β-D-glucans[3].

In studies of pulses, cellular integrity is a critical factor underpinning their low glycaemic index[4]. The tendency of leguminous cells to separate is commonly observed in hydrothermally processed chickpeas and many other pulses, but not in beans that exhibit hard-to-cook defects[5]. Cell separation is possible in tissues where the middle lamella is held together largely by non-covalent cross-linked pectic polysaccharides and results from solubilization and/or heat-catalysed depolymerization of pectin in the middle lamella of contiguous cells under certain processing conditions[3]. This weakening of intercellular adhesions means that hydrothermally treated legume cotyledon cells can separate from each other during mastication. The resulting intact cells that constitute the food bolus can therefore be the main structural entity that enters the gastrointestinal tract (GIT)[6]. Micrographs of intact, starch-containing plant cells from white haricot beans and mature peas in human ileal fluid[7,8] confirm that cellular structures from leguminous plant tissues with type I cell walls persist to some extent in the upper GIT. In contrast, wheat endosperm tissues have type II cell walls and do not cell separate when hydrothermally processed. Wheat grains fracture following mechanical processing such that the proportion of starch that remains encapsulated within plant cells is likely to depend on the cell volume and particle size of the wheat tissue[9]. Although wheat is conventionally dry milled to a subcellular flour before cooking and consumption, we previously showed that large macroparticles of wheat endosperm tissue can remain intact during transit through the upper GIT, leading to an attenuation of postprandial glycaemia compared with subcellular flour[10].

Several previous in vitro digestibility studies have observed lower starch digestibility associated with intact cells or tissues of cooked legumes[11–15] and cereals[15–17]. One possibility is that the cell walls, which are not digested by mammalian enzymes of the upper GIT, exist as physical barriers to delay enzyme ingress. The degree of penetration of digestive enzymes through cell walls is likely to be influenced by many factors, such as cell wall thickness, density and composition, the size and number of cell wall pores including plasmodesmata, and processing treatments[2,6,18]. Assessing the permeability of cereal endosperm cells, which can remain intact within food macroparticles, is difficult, but indirect microscopic evidence suggests that amylase can cross the cell wall[10]. An additional mechanism of interest is the proposed role of the cell wall in limiting starch gelatinization and thereby starch susceptibility to amylase digestion[19]. Observations of distorted granular swelling[11] and quantitative studies showing limited gelatinization of starch[19] within legume tissues provide evidence for this mechanism; however, it is unclear whether this can be rate limiting.

Through a series of comparative structure–function studies of chickpea and wheat, we elucidate the mechanisms by which cell wall properties influence starch bioaccessibility. The proposed role

[1]Biopolymers Group, Departments of Biochemistry and Nutritional Sciences, Faculty of Life Sciences and Medicine, King's College London, London, UK. [2]Quadram Institute Bioscience, Norwich, UK. [3]Department of Chemical, Biological, Pharmaceutical and Environmental Science, University of Messina, Messina, Italy. [4]Present address: Quadram Institute Bioscience, Norwich, UK. ✉e-mail: cathrina.edwards@quadram.ac.uk; peter.r.ellis@kcl.ac.uk

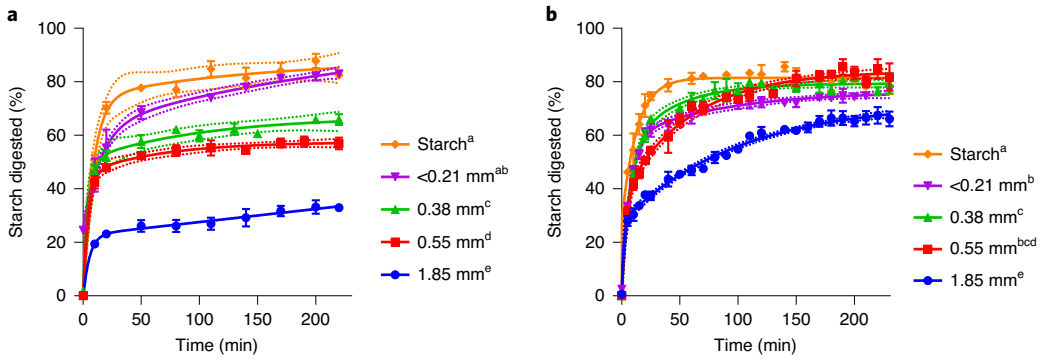

Fig. 1 | Particle size and starch digestion kinetics. a,**b**, Effect of dry-milled particle size on starch digestibility in hydrothermally cooked chickpea (**a**) and durum wheat (**b**), as investigated in chickpea cotyledon and durum wheat endosperm tissue particles, respectively, and in starch extracted from these tissues. All samples were dry milled and sieved to obtain distinct size fractions, then hydrothermally processed at 100 °C for 1 h 25 min before incubation with pancreatic α-amylase (~0.17 U per mg starch). Starch amylolysis products were quantified by Prussian blue assay and expressed as maltose equivalents. The concentration of reducing sugars before the addition of pancreatic amylase was negligible. The legends indicate median particle sizes. Different superscript letters indicate a significant difference in starch digestibility between particle size fractions within chickpea or durum wheat ($P < 0.05$; mixed-effects model analysis of variance with Tukey's post-hoc test). The values are the means of triplicates and error bars represent s.e.m. The curves were obtained by least-squares regression to two-phase association equations, and 95% confidence bands (dotted lines) show the likely location of the true curve. $R^2 > 0.99$ for all curves.

of encapsulating cell walls in impeding intracellular starch gelatinization and/or enzyme access was examined in digestibility studies supplemented with microscopy of samples taken before and after processing and digestion. The dynamic gastric model (DGM) and static duodenal model (SDM) were used in combination to provide a physiologically relevant simulation of the human stomach and duodenum, respectively[20,21]. Deeper insight of the properties of these different cell wall types, particularly their behaviour during processing and digestion, can improve our understanding of the mechanisms by which different sources of dietary fibre influence public health. Also, this could lead to the development of more effective and palatable forms of dietary fibre for improving glucose homeostasis in individuals with (or at risk for) type 2 diabetes.

Results

A series of in vitro digestibility studies provided new insight into mechanisms by which plant tissue structure influences starch bioaccessibility from chickpea cotyledon and durum wheat endosperm.

Lower digestibility of cell-wall-encapsulated starch. Chickpea and durum wheat were dry milled to obtain different-sized fractions and then hydrothermally processed to inactivate endogenous amylase before determination of starch digestibility (Fig. 1). The larger particles, which contained more cell-wall-encapsulated starch, had the lowest starch digestibility. As the cellular integrity of the tissue was further disrupted through reductions in particle size, both the rate and proportion of starch digested by amylase increased. In chickpea materials (Fig. 1a), increased particle size, and thereby greater cell wall encapsulation of starch, limited the extent of starch digestion (mean percentage digested (±s.e.m.) after 220 min = 82.5 ± 1.5, 82.9 ± 0.3, 65.9 ± 2.0, 57.0 ± 2.2 and 33.0 ± 0.9% for starch and particle size fractions of <0.21, 0.38, 0.55 and 1.85 mm, respectively), which plateaued within 60 min of amylolysis. In durum wheat, differences in digestion rate were evident, but the extent of starch digested after 230 min (~80%) was similar for all durum wheat size fractions except the largest 1.85 mm fraction, where 66 ± 2.7% of the starch had been digested and had not yet reached a plateau (Fig. 1b). These differences suggest that chickpea cell walls hinder amylase access to a greater extent than the cell walls of wheat. The starch digestibility profiles of boiled starch extracted from chickpea and wheat were similar, thus confirming that the kinetic effects are attributed to properties of the cellular tissue, rather than the starch structure.

Cell integrity after homogenization limits starch digestibility. We investigated how the two plant tissues behave after hydrothermal cooking (100 °C) when subjected to high shear, and the extent to which this influences starch digestibility and tissue microstructure. The largest of the wheat and chickpea macroparticles (1.85 mm) prepared by dry milling (containing the highest proportion of encapsulated starch) were prepared as a porridge and homogenized or left intact before the starch amylolysis assay.

Micrographs show the internal structural integrity of intact chickpea (Fig. 2a) and durum wheat macroparticles (Fig. 2b) after they have been cooked but not homogenized. The chickpea and wheat tissues predominantly comprised intact starch-rich cells of cotyledon and endosperm tissues, respectively, with some ruptured cells evident at the particle edges (Fig. 2a,b). Chickpea cotyledon cells had thicker walls (~1–2 µm, estimated from micrographs) than wheat endosperm cells (≤1 µm) and a rounded appearance, consistent with solubilization of middle lamellar pectin and weakening of cell–cell adhesion during hydrothermal processing. Durum wheat endosperm cell walls were visibly thinner and less defined (~0.6–1.0 µm, estimated from micrographs) and the endosperm cells were more angular and tightly associated. After 2 h of in vitro digestion, chickpea cells at the particle edge and core appeared intact, with starch enclosed (Fig. 2c), whereas starch-containing cells of durum wheat endosperm were still present at the particle core (Fig. 2d). After 6 h of in vitro digestion, the overall structural integrity of the intact chickpea macroparticles remained largely unchanged (Fig. 2e). Wheat endosperm cells near the particle edge were ruptured and starch from the cells was presumed to be digested (Fig. 2f). Wheat endosperm cells near the particle core were intact and the numbers of intracellular starch granules appeared to be reduced in the outermost cell layers, although the quantitative data in Fig. 3 provide a more reliable indication of starch digestion.

The effect of homogenization on tissue structures and starch digestibility is shown in Fig. 3. The micrographs reveal that when homogenization treatment was applied to intact macroparticles of hydrothermally processed chickpea cotyledon (Fig. 3a) the tissue

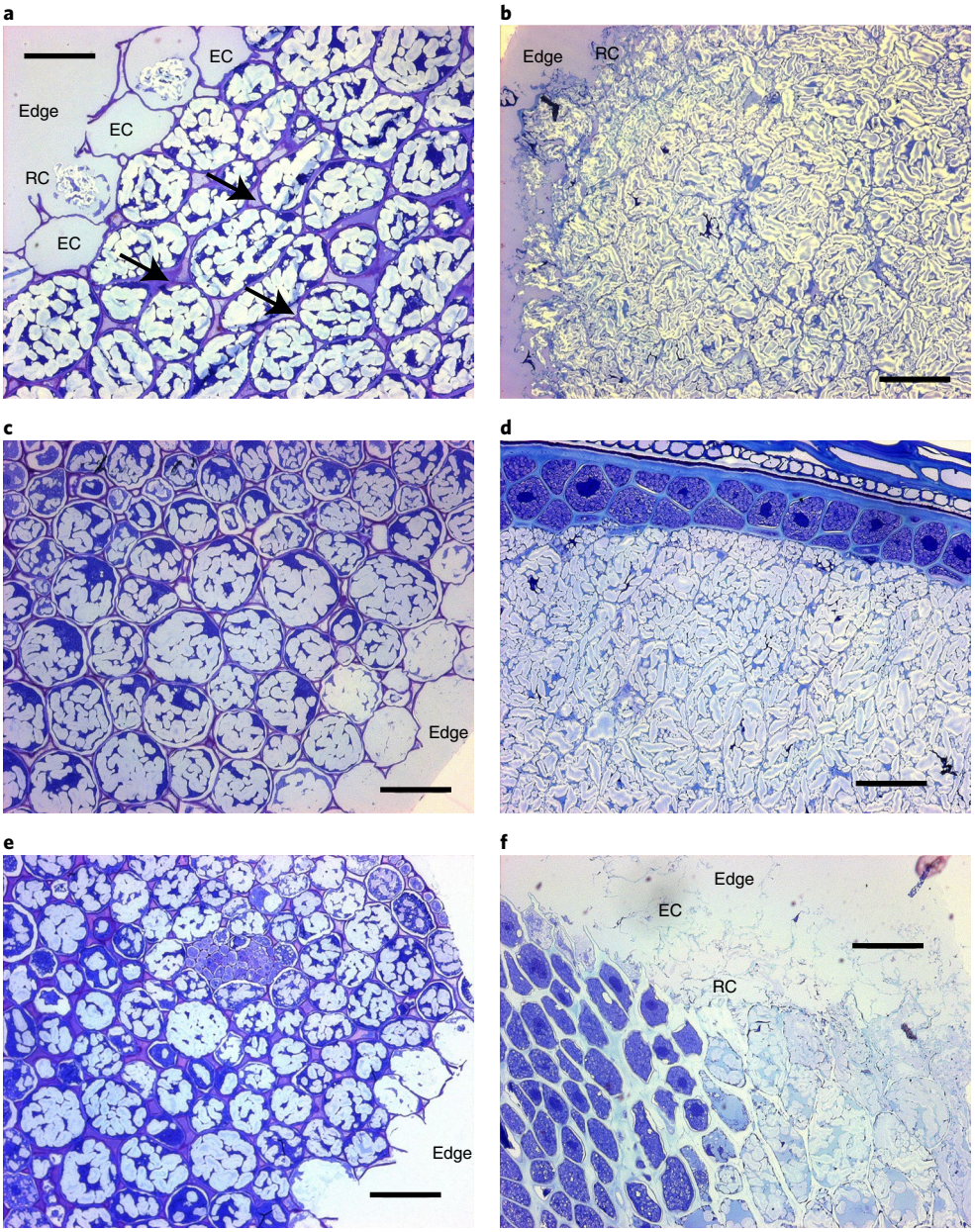

Fig. 2 | Microstructure of hydrothermally cooked intact tissue macroparticles. a–f, Light micrographs of cross-sections of chickpea (**a**, **c** and **e**) and wheat macroparticles (**b**, **d** and **f**) before digestion (**a** and **b**) and 2 h (**c** and **d**) and 6 h after digestion (**e** and **f**). Cross-sections were cut to 0.5 µm thickness and stained with toluidine blue (1% wt/vol with 1% wt/vol sodium borate). In the micrographs captured before digestion (**a** and **b**), the cell walls are seen to surround intracellular starch within the intact tissue, with some ruptured cells (RC) and/or empty cells (EC) present on the particle edges (that is, the fractured surface created by dry milling). The arrows indicate some of the areas where weakening of intercellular linkages has occurred. The internal structure and edges of chickpea tissue examined after 4 h of in vitro digestion (**c**) did not appear to be altered. After 2 h of digestion, wheat starch was still evident within many endosperm cells, particularly those in close proximity to the aleurone layer or crease (**d**). The appearance of chickpea tissue remained unchanged after 6 h (**e**), whereas wheat endosperm cells near the particle edges had collapsed and/or had been eroded (edge) after 6 h (**f**). Scale bars, 50 µm.

became disrupted and individual cells separated, with only a few cells showing evidence of structural damage or cell wall rupture. Most of the cotyledon cells remained intact, with the starch encapsulated by the cell walls. When the same homogenization treatment was applied to the macroparticles of hydrothermally cooked intact wheat endosperm, it caused extensive cell and tissue structure damage, exposing partially swollen starch granules and other intracellular debris (Fig. 3b). No intact endosperm cells or tissue clusters were detected in these wheat samples; only protein fragments and some bran residue (that is, the pericarp, testa and aleurone layers) were seen against a background of mostly swollen starch granules. In micrographs taken after 6 h of digestion with amylase, intact chickpea cells remained (Fig. 3c) and had a similar appearance to the cells in the sample collected before digestion, whereas the free starch from ruptured cells appeared to have been digested. In the image of the homogenized and digested wheat endosperm, there was little evidence of any starch remaining, at least not in the form of identifiable starch granules (Fig. 3d).

Starch digestibility curves showing the digestion of hydrothermally cooked chickpea and wheat macroparticles that had been

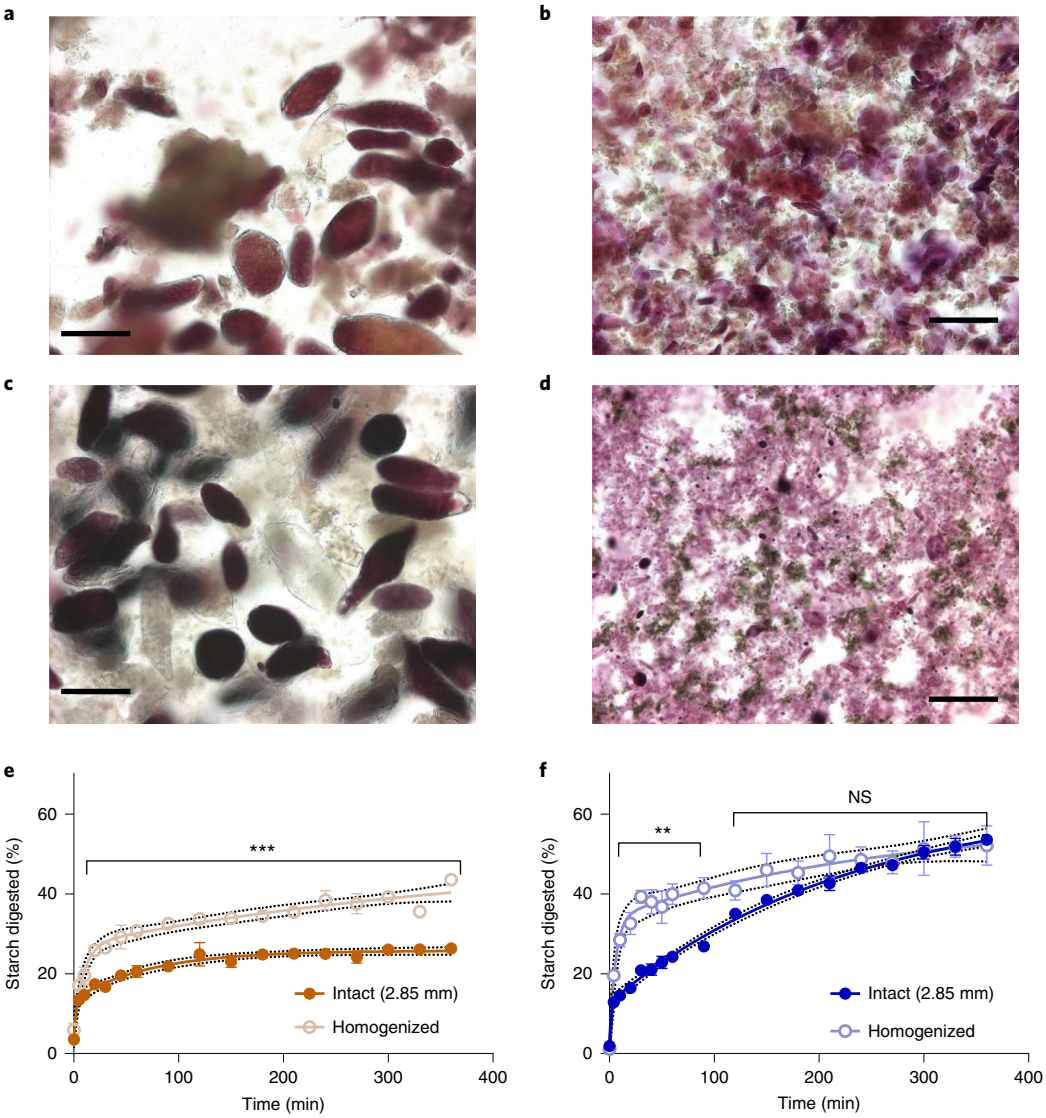

Fig. 3 | Homogenization of cooked macroparticles and starch digestibility. a–d, Light micrographs of homogenized chickpea (**a** and **c**) and wheat macroparticles (**b** and **d**) captured before (**a** and **b**) and after 6 h of in vitro digestion (**c** and **d**), stained with 2.5% Lugol's iodine solution. Intact macroparticles (1.85 mm) of chickpea cotyledon and durum wheat endosperm were hydrothermally cooked before homogenization for 30 s at 16.4×10^3 r.p.m. Homogenization caused cell separation in chickpea (**a**) and cell rupture in wheat (**b**). After 6 h incubation with amylase, the chickpea cells remained intact (**c**) while starch granules released from chickpea and wheat cells by homogenization pre-treatment had been digested (**c** and **d**). **e**,**f**, Starch digestibility curves showing the progress of starch digestion of hydrothermally cooked intact and homogenized chickpea (**e**) and wheat macroparticles (**f**). The digestions were performed in quadruplicate, and mean values ± s.e.m. are presented. Significant differences (as determined by paired *t*-test) between starch digestions from intact and homogenized particles are indicated (**$P < 0.01$; ***$P < 0.001$). NS, not significant ($P > 0.05$). The curves were obtained by least-squares regression to two-phase association equations, and the 95% confidence bands (dotted lines) show the likely location of the true curve. The R^2 values were 0.95 and 0.92 for intact and homogenized chickpea, and 0.98 and 0.81 for intact and homogenized durum wheat, respectively. Scale bars, 50 µm.

homogenized compared with structurally intact (non-homogenized) controls are shown in Fig. 3e,f. Homogenization of chickpea materials produced a significant increase in the extent of starch digestion, but the intact chickpea samples showed persistently lower levels of digestion even after 6 h incubation (Fig. 3e). Similarly, homogenization of cooked durum wheat macroparticles led to a significant increase in the rate of starch digestion (Fig. 3f); however, the same amount of starch (~50%) had been digested after 6 h in both the intact and homogenized wheat samples.

Structure regulates starch bioaccessibility in the stomach and duodenum. The purpose of these experiments was to study starch bioaccessibility and digestion, as well as the tissue and cell microstructure of chickpeas and durum wheat, prepared as porridge test meals, under simulated physiological conditions of oral, gastric and duodenal digestion. For the chickpea experiments, the main objective was to determine the effects of freeze milling on the digestibility and structural integrity of separated chickpea cells. For the wheat experiments, the main objective was to determine the effects of particle size of wheat macroparticles on starch bioaccessibility and digestion, and also to monitor microstructural changes.

Chickpea porridge. Starch digestion from chickpea porridges with contrasting cellular integrity is shown along with micrographs in

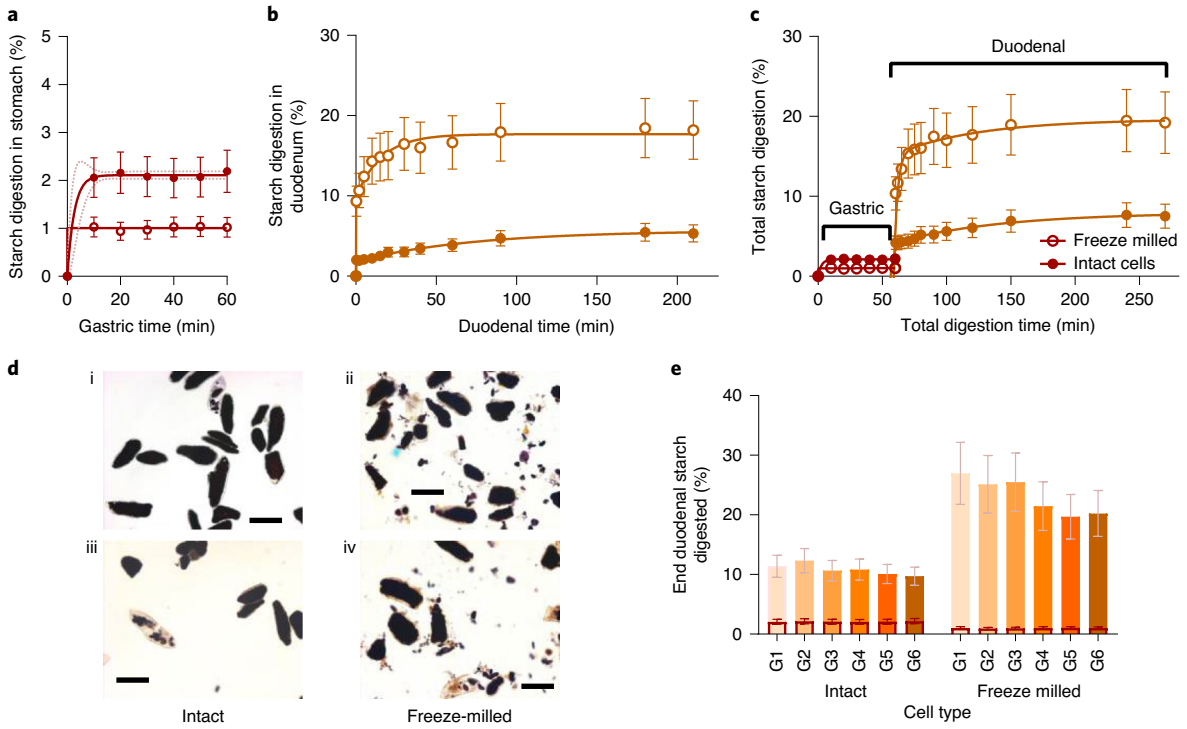

Fig. 4 | Gastric and duodenal digestion of chickpea porridges with contrasting cell structure. Chickpea porridges made with intact or freeze-milled chickpea cells were digested using the DGM followed by the SDM. **a**–**c**, Starch digestibility curves showing the percentage of total starch that was digested at each time point from chickpea porridge made from intact (filled circles) or freeze-milled cells (open circles) in the stomach (**a**), duodenum (**b**) or both (**c**). The profiles in **b** and **c** are of samples subjected to 60 min of gastric residence, wherein the gastric baseline has been subtracted (**b**) or included to give the total amount of starch amylolysis (**c**). Curve fits were obtained by least-squares regression to one-phase (**a**; $R^2 > 0.99$) or two-phase (**b**; $R^2 > 0.99$) association equations, with 95% confidence intervals shown as error bars. **d**, Micrographs of intact (left) and freeze-milled porridge (right) captured before (top) and after duodenal digestion (bottom). All micrographs were stained with iodine/potassium iodide. Scale bars, 100 μm. **e**, Clustered column chart showing the percentage of total starch that was digested at the end of the duodenal phase, clustered by cell treatment type (intact versus freeze milled), and with a separate column for each gastric residence time (10, 20, 30, 40, 50 and 60 min, labelled G1, G2, G3, G4, G5 and G6, respectively). The overlaid columns with a dark border represent the extent of starch released from each sample during the gastric phase. All experimental points represent the mean of three determinations obtained from one (freeze milled) or two (intact) simulated digestion runs. The error bars represent 20% s.e.m.

Fig. 4. In the gastric phase, the amount of reducing sugars released from starch by human salivary amylase was minimal, accounting for 1–2% of the total starch present in the porridge meals. The concentration of reducing sugars remained constant between 10 and 60 min of gastric incubation and there was no evidence that starch digestion (by salivary amylase) continued during gastric digestion of either porridge type (Fig. 4a).

Once in the duodenal phase, starch amylolysis in the porridge made from freeze-milled chickpea cells progressed rapidly within the first 15 min, whereas amylolysis in the porridge made from intact cells progressed more slowly and to a lesser extent (Fig. 4b). For the porridge prepared from intact cells, there was no difference between the duodenal digestion profiles of samples that had different gastric residence times, indicating that the gastric phase had no effect on the susceptibility of starch in these porridges to subsequent duodenal amylolysis (Supplementary Fig. 1). However, for porridge made from freeze-milled cells, there was a tendency for samples that had ≤20 min in the gastric phase to be more susceptible to amylolysis during subsequent duodenal digestion (Supplementary Fig. 1).

The progress of total starch amylolysis throughout gastric (60 min) and subsequent duodenal digestion is shown for both porridge types in Fig. 4c. The starch bioaccessibility from porridge made of intact cells of chickpea cotyledon was very low, with less than ~10% of the starch becoming digested, whereas up to 26% of the starch in the porridge made from freeze-milled cells was digested. For both porridge types, the duodenal phase was the predominant site of starch amylolysis. Micrographs (Fig. 4d) revealed that a high proportion of cells remained intact despite the freeze-milling treatment, and that these cellular structures with encapsulated starch remained intact after duodenal digestion.

The total amount of starch digested at the end of the duodenal phase for each gastric residence time and porridge type is shown in Fig. 4e. The total extent of starch digested was higher for the porridge made with freeze-milled cells compared with that made with intact cells. However, the majority of starch in both porridge types remained undigested, with around 90 and 75% of starch in the porridges made from intact and freeze-milled cells, respectively, remaining at the end of the duodenal phase. A slight reduction in the total extent of digestion was observed for samples retained in the gastric phase for a longer period. This effect was more pronounced in the porridge made from freeze-milled cells, which could reflect the retention of larger particles (intact cells, which have a lower susceptibility to amylolysis than free starch) in the DGM.

Wheat porridge. Starch digestion from wheat porridges made with different particle sizes of endosperm is shown together with micrographs in Fig. 5. Starch digestion by salivary amylase continued throughout the gastric phase, and the gastric starch digestion profiles (Fig. 5a) show a similar time-dependent increase in starch amylolysis for all size fractions of wheat used for preparing the porridge.

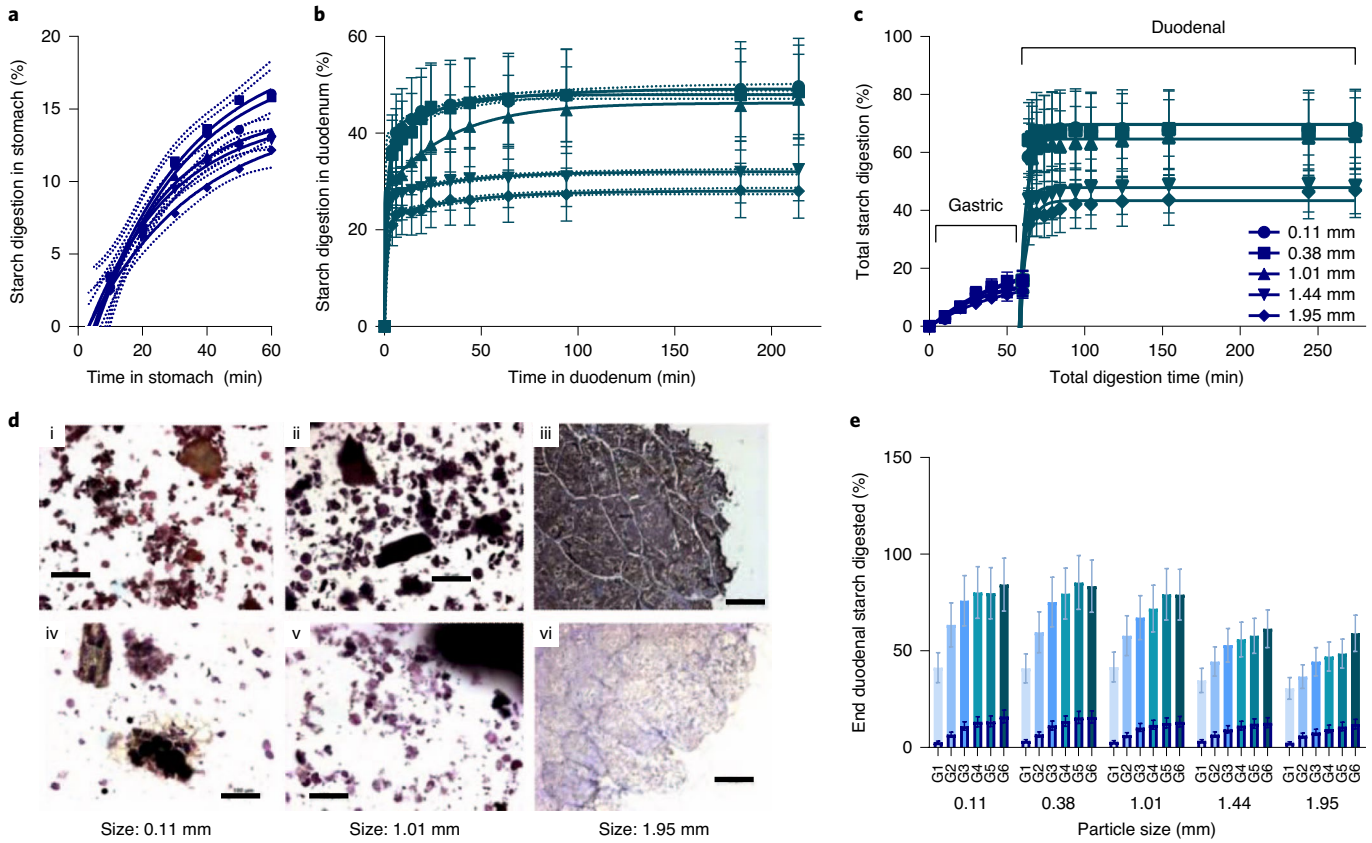

Fig. 5 | Gastric and duodenal digestion of wheat porridges with contrasting particle sizes. Wheat porridges made with different particle size fractions of milled endosperm were digested using the DGM followed by the SDM. **a**–**c**, Starch digestibility curves showing the percentage of total starch that was digested at each time point from wheat endosperm porridge with contrasting particle sizes (circles, 0.11 mm; squares, 0.38 mm; upward-pointing triangle, 1.01 mm; downward-pointing triangle, 1.44 mm; diamond, 1.95 mm) in the stomach (**a**), duodenum (**b**) or both (**c**). The profiles in **b** and **c** are of samples subjected to 60 min of gastric residence, wherein the gastric baseline has been subtracted (**b**) or included to give the total amount of starch amylolysis (**c**). Curve fits were obtained by least-squares regression to one-phase (**a**; $R^2 > 0.98$) or two-phase (**b**; $R^2 > 0.99$) association equations, with 95% confidence intervals shown as error bars. **d**, Micrographs of particle size 0.11 mm (left), 1.01 mm (middle) and 1.95 mm (right) captured before duodenal digestion (top left and top middle), during mid-gastric digestion (top right) and after duodenal digestion (bottom three panels). All micrographs were stained with iodine/potassium iodide. Scale bars, 100 μm. **e**, Clustered column chart showing the percentage of total starch that was digested at the end of the duodenal phase, clustered by particle size, and with a separate column for each gastric residence time (10, 20, 30, 40, 50 and 60 min, labelled G1, G2, G3, G4, G5, and G6, respectively). All experimental points represent the mean of three determinations obtained from three simulated digestion runs. The error bars represent 20% s.e.m. The overlaid columns with a dark border represent the starch released from each sample during the gastric phase.

After 60 min in the gastric phase, up to 16% of the total starch in the wheat porridges had been digested. Once in the duodenal phase, starch amylolysis progressed rapidly within the first 4 min and plateaued within 60 min for all size fractions (Fig. 5b). Under duodenal conditions (not including the contributions from the gastric phase), on average, 48% (range = 34–54%) of the total starch in the wheat porridges made from smaller particle size fractions (median size = 0.11, 0.38 or 1.01 mm) was digested, whereas an average of 30% (range = 25–35%) of the total starch in the larger size fractions (median size = 1.44 or 1.95 mm) was digested. There was a general tendency for samples that had ≤20 min of gastric residence to be digested in the duodenal phase more slowly than samples with >20 min of gastric incubation, suggesting that samples with a short gastric residence were less susceptible to subsequent duodenal amylolysis (Supplementary Fig. 2). Progression of starch amylolysis throughout gastric (60 min) and duodenal digestion is shown in Fig. 5c. For all size fractions, gastric starch amylolysis (by residual salivary α-amylase) made some contribution to total amylolysis, but the majority of starch amylolysis occurred within the first 4 min of exposure to pancreatic α-amylase in the duodenal model. On average, the proportion of total starch digestion attributed to the gastric phase was about 19% of the total starch amylolysis (range = 7–26%), where the values at the lower end of this range originate from samples that experienced shorter gastric residence times. The remaining 81% (range = 74–93%) of the total starch amylolysis occurred within the duodenal phase and mostly within the first 4 min (as shown in Fig. 5c). Micrographs (Fig. 5d) show that starch had been digested from exposed granules (sizes = 0.11 and 1.01 mm) and from the peripheral cells of larger macroparticles (size = 1.95 mm) in samples recovered from the duodenal phase. The total amount of starch digested at the end of the duodenal phase for each gastric residence time and particle size is shown in Fig. 5e. The total extent of digestion increased with gastric residence time and decreasing particle size.

Discussion

These studies were performed to gain insight into the underlying mechanisms of starch digestion in edible plants; specifically, chickpea cotyledon (with type I primary cell walls) and durum wheat endosperm (with type II cell walls). Identical mechanical treatment

(dry milling and homogenization) of these tissues had different effects on starch bioaccessibility, with implications for glycaemic responses and the nature and amount of resistant starch that is delivered to the colon. These studies highlight the importance of tissue fracture properties and cell wall permeability as key mechanisms by which dietary fibre influences starch bioaccessibility.

In wheat, the final amount of starch digested in different-sized fractions was the same, but the time to reach the end point was dependent on particle size. In contrast, in chickpeas, size greatly affected the final amount of starch digested. These results are consistent with predictions from our previous kinetic studies of early stages of digestion of plant material[15].

The marked disparity in digestibility profiles between wheat and chickpeas is probably explained by intrinsic differences in the cell tissue properties, especially the permeability of cell walls to amylase diffusion. Digestion of intracellular starch from wheat endosperm indicates that the cell walls were permeable to α-amylase. In contrast, digestion of starch from chickpea tissue was limited to ruptured cells on the fractured surface of particles, and is consistent with reports of low starch amylolysis from intact leguminous plant cells[11–13,22,23]. Restricted amylolysis is a consequence of low permeability to amylase (cell wall barrier mechanism) and/or intracellular starch being less susceptible to amylolysis (restricted gelatinization mechanism). The higher dietary fibre values of chickpea flour reflect their thicker cell walls (which account for ~5–6% of the cotyledon tissue mass) compared with wheat endosperm flour (which comprises ~2–3% of cell wall material)[24].

The relative contributions of these two mechanisms were investigated further in studies where hydrothermally cooked macroparticles were disrupted by homogenization (blending) treatment. These studies revealed extensive cell fracture in wheat (that is, the cell wall barrier was removed) and the starch was digested more rapidly than in control samples with intact tissue structure. However, even after 6 h of incubation with α-amylase, 50% of the starch in both the intact and homogenized wheat samples remained undigested, suggesting that starch cooked inside this plant matrix retained some ordered structure[19]. For chickpeas, the tissue separated into individual cells with intact cell walls so that access to intracellular starch was impeded.

The contrasting fracture/separation behaviour of hydrothermally cooked durum wheat and chickpea tissues has implications for the type of cell wall structures that digestive enzymes are likely to encounter in vivo. Under simulated digestive conditions of the stomach and duodenum, chickpea cells remained intact and the bioaccessibility of starch from these cells was very low.

In hydrothermally cooked wheat endosperm, larger particles of tissue remained intact throughout simulated gastric and duodenal digestion, with a progressive loss of starch from intact cells near the particle periphery towards the core. This is consistent with digestion patterns observed from large endosperm particles recovered from the terminal ileum of human participants in an in vivo study, where reduced bioaccessibility of starch in endosperm macroparticles significantly attenuated postprandial glycaemic and insulinaemic responses[10].

The physiological conditions simulated in DGM and SDM digestion models are considered to be more representative than direct amylolysis assays[20,21]. The rate and extent of amylolysis is recognized as being relevant for predictions of glycaemic responses[25,26], but the acidity and mixing of the stomach, and activities of other enzymes (for example, pepsin and trypsin digestion of proteins), have been suggested to influence subsequent duodenal amylolysis. We observed that salivary amylase (added during the oral phase) continued to digest wheat starch throughout the gastric phase, accounting for ~20% of the total starch amylolysis in wheat, but digested <2% of the starch from chickpea cells. Thus, the mechanisms by which cell walls affect starch digestibility in the duodenal phase are equally relevant to the oral digestion. Gastric residence in excess of 20 min was associated with a slight change in the rate and extent of subsequent duodenal starch amylolysis (an increase for wheat and a decrease for chickpeas). However, no changes in cell wall or tissue structures were evident from the microscopy of samples recovered from the DGM and it is noteworthy that, due to the gastric sieving, this difference could reflect the dissimilar nature of material being released into the duodenal phase. Nevertheless, most starch digestion from these samples occurred within the early stages of duodenal digestion.

From a nutritional perspective, the reductions in the rate and extent of starch bioaccessibility observed in our in vitro studies would be expected to produce an attenuation in glycaemic and insulinaemic responses in vivo, and the resistant starch remaining at the end of simulated upper gastrointestinal digestion would be available for fermentation by the colonic microbiome. Thus, processing treatments (for example, combinations of dry milling, cooking and blending) that have different effects on the cellular integrity and cell wall permeability of starch-storage tissues are highly relevant to our understanding of the physiological effects of dietary fibre from legumes and cereals. Such mechanistic understanding has potential for optimizing the health benefits of dietary fibre components of foods for gastrointestinal health, prevention of type 2 diabetes and weight management. Our studies emphasize the crucial importance of structural integrity of dietary fibre in explaining physiological mechanisms of fibre. Inclusion of the innovative DGM in combination with the SDM has provided a physiologically relevant simulation of the proximal GIT conditions to demonstrate the contrasting behaviour of legume and wheat tissues during digestion. In particular, the DGM, which was employed to mimic both biochemical and mechanical processes of gastric digestion in a realistic time-dependent way, has shown that gastric conditions enhance starch digestion in wheat but not chickpea tissue. These results raise questions about fibre supplementation and health claims when the physical form of fibre is not retained during food processing. Moreover, this work highlights the problems of relying only on chemical analysis of dietary fibre for characterizing the physiological properties of fibre in plant foods, particularly when this information is used to interpret mechanistic data and the results of human studies. Further research on the supramolecular structure, mechanical properties and porosity of cell walls would add to our understanding of the physiological and clinical effects of dietary fibre[2]. Such insight could also help the food industry to design more effective fibre-rich food ingredients and products.

Methods

Materials. Dried seeds of chickpea *C. arietinum* L. (Russian variety) were donated by Poortman. Samples of durum wheat *T. durum* L. (Svevo variety) were provided by Millbo. Starch was isolated from these grains, purified and dried, as described previously[15], for use as a reference material in some experiments. Milled macroparticles of a defined size were prepared from the starch-rich storage tissue of each species. Chickpeas were soaked overnight and then manually de-hulled while wet to remove the testa, and finally left to dry at ambient temperature until the weight had stabilized and moisture of <10% was reached. Durum wheat grains were de-branned for 2 min (Satake TM-05C de-branner equipped with a medium abrasive roller (No. 40); roller speed = 1,450 r.p.m.) to remove the outer bran layers. The dry chickpea cotyledon and wheat endosperm tissues were then roller milled (Satake test roller mill STR-100 equipped with 4.134 flutes cm^{-1} break rolls; 250 mm diameter) using a sharp-to-sharp disposition to achieve geometrically well-defined macroparticles. The milled material was separated into particle size fractions as denoted in the following sections by the median size based on sieve apertures.

Proximate analysis. Proximate analysis (protein, lipid, dietary fibre (measured using a set of methods developed by the Association of Official Analytical Chemists), ash (total mineral content), moisture and carbohydrate by difference) of durum wheat and chickpea materials was done by Premier Analytical Services (The Lord Rank Centre, High Wycombe, UK), as described previously[10]. The total starch content of these materials was measured directly, using a modified version of the Association of Official Analytical Chemists' 996.11 Total Starch procedure, with Megazyme Total Starch Assay kit reagents (Megazyme International Ireland),

as described in full elsewhere[10]. Milled chickpea fractions contained 23 g protein, 22.6 g dietary fibre, 5.3 g lipid, 2.8 g ash, 8.7 g moisture and 37.5 g carbohydrate (by difference) per 100 g wet weight. Milled durum wheat endosperm contained 10.7 g protein, 6.5 g dietary fibre, 1.7 g lipid, 0.9 g ash, 9.9 g moisture and 70.2 g carbohydrate (by difference) per 100 g wet weight. The total starch content of milled size fractions was 40 ± 2% for chickpea and 63 ± 2% for durum wheat.

Light microscopy. Samples for light microscopy were collected before and after digestion procedures. Samples of intact macroparticles were fixed overnight in modified Karnovsky's fixative (1.6% vol/vol formaldehyde and 2% vol/vol glutaraldehyde), rinsed in 0.1 M sodium cacodylate buffer (pH 7.2) and then dehydrated through a graded ethanol series. Samples were embedded in LR White Resin (62662; Fluka) and polymerized (cured) at 60 ± 2 °C for 24 h. Sections (0.5 or 1 µm) were cut using a glass knife mounted on an ultramicrotome (Ultracut E; Reichert Jung), dried and stained with 1% (wt/vol) toluidine blue in 1% (wt/vol) sodium borate or Lugol's iodine (2.5% iodine with 5% potassium iodide). Sections (0.5–1 µm) were viewed using a Leica Zeiss AxioSkop-2 MOT Plus light microscope and images were captured using a Zeiss AxioCam HRc camera and AuxioVision version 3.1 microscope software. Micrographs of homogenized samples were obtained by immediate examination of sections without prior fixation.

Starch amylolysis assay. The susceptibility of chickpea and wheat materials to starch amylolysis was assayed following a protocol that has been described previously[15]. In brief, 50 ml tubes containing phosphate buffered saline (PBS) suspensions of materials for testing were incubated in a water bath at 37 °C for 20 min. A blank aliquot (200 µl) of the solution was then removed to a microfuge tube and mixed with an equal volume of ice-cold 0.3 mol l^{-1} Na_2CO_3 (stop solution). To start the amylolysis reaction, porcine pancreatic amylase (from high-purity enzyme A6255 obtained from Sigma–Aldrich; Enzyme Commission number 3.2.1.1) was added immediately to the suspensions, to achieve a ratio of 2.3 nmol l^{-1} amylase (~0.17 U) per mg starch in the final digestion mixture. The sample tubes were incubated on a rotary shaker at 37 °C for the duration of the assay (up to 6 h). Aliquots (200 µl) of the digestion mixture were subsequently collected at regular time points into an equal volume of ice-cold stop solution, to terminate amylolysis. Microfuge tubes from each sampling occasion were then centrifuged at 16,200*g* (Heraeus Pico; Thermo Fisher Scientific) for 6 min to spin down any starch remnants, and the supernatant was collected and frozen at −20 °C for subsequent analysis. Starch hydrolysis products (reducing sugars; predominantly maltose and maltotriose) in the supernatant were quantified using a Prussian blue assay method[15], which provided reliable measurements of low concentrations of reducing sugars.

Starch digestion kinetic study of dry-milled plant tissues. The experiment was performed on dry-milled plant tissue from chickpea and wheat with different particle sizes, and therefore different ratios of surface to encapsulated starch, to gain insight into the effect of tissue structure and cell encapsulation on starch digestion kinetics. Four different size fractions (median size = 1.85, 0.55, 0.38 or <0.21 mm (flour)) of dry-milled chickpea (3.15 g) and durum wheat (2.10 g) tissue and starch isolated from these materials were each weighed into 50-ml Falcon tubes so that each tube contained 1,260 ± 2 mg starch. The sample in each tube was suspended in 30 ml PBS. All samples were then hydrothermally processed at 100 °C for 1 h 25 min with intermittent stirring, then subjected to the amylolysis procedure described above to obtain starch digestibility profiles for each size fraction. The experiment was repeated three times.

Starch digestibility study of intact and homogenized plant tissues. This experiment compared the starch digestibility of macroparticles of chickpeas and durum wheat that had been hydrothermally treated as intact tissue then homogenized, to provide insight into the behaviours of different tissue types and implications for the role of cell walls as physical barriers and restrictors of starch gelatinization.

Coarse macroparticles (median size = 1.85 mm) of chickpea (3.15 g) and durum wheat (2.10 g) were each weighed into 2 ml × 50 ml Falcon tubes so that all tubes contained the same amount of total starch (1,260 ± 2 mg per tube). The duplicate tubes were prepared, cooked and tested in parallel (as described below), but only one was homogenized, leaving the structures of the plant tissue macroparticles in the other tube intact. The experiment was repeated four times, with chickpea and wheat samples tested in each experimental run using the same assay.

The chickpea samples were left to soak in 7 ml PBS at room temperature (~22 °C) overnight and then boiled for 40 min, whereas wheat was soaked at room temperature for 50 min and then boiled for 10 min. Both sample types were boiled in soaking liquor to keep the starch concentration constant. The two different hydrothermal regimens used ensured that each material type was cooked to a texture that would be considered palatable for human consumption.

After cooking, the samples were kept at 37 °C for 10 min. From each pair of tubes, the macroparticles of one tube were homogenized (see below) while the other tube was left untreated so that the macroparticles remained intact. Homogenization was carried out using an IKA T25 Digital Ultra-Turrax by immersing the Ultra-Turrax probe in the tube and homogenizing the content for 30 s at 16.4 × 10^3 r.p.m. Residual material from the Ultra-Turrax probe was rinsed back into the tube with an additional 3 ml PBS. In parallel, the same volume was also added to the untreated sample tube containing the intact macroparticles.

All tubes were incubated at 37 °C in a water bath for a further 5 min, diluted to a final total volume of 30 ml with PBS (at 37 °C) and then submitted to the starch amylolysis assay procedure (described above) to monitor starch digestion over 6 h. Digestibility curves were fitted to the data points through nonlinear regression.

Digestions via the DGM and SDM. This study employed the use of physiologically relevant digestion systems that simulate the biochemical and mechanical conditions of the GIT, including oral, gastric (DGM) and duodenal (SDM) phases.

Chickpea porridge. Chickpea porridges were prepared from dried separated cells (containing 48.2 g starch and 10 g moisture per 100 g dry matter), which were either left intact or freeze milled to disrupt the cellular integrity. For freeze-milled cells, the dried chickpea cells were subjected to 2 × 30 min of freeze milling at ten cycles per second (6970D Freezer/Mill; SPEX SamplePrep), to induce cell rupture and release intracellular starch. To prepare the porridge meals, 70 g dried chickpea cells (either freeze milled or intact) were soaked in 180 ml of water overnight and then cooked for 20 min with the addition of another 170 ml of water, following the same process as described for wheat. After cooking, the total weight of the porridge was re-adjusted to 350 g by the addition of water to make up for evaporative losses. The porridge was then digested using the DGM and SDM.

One cooked portion of chickpea porridge (~350 g) contained 35.0 g of potentially available carbohydrate (of which 34.9 g was starch and 0.1 g was total sugars), 9.8 g dietary fibre, 14.8 g protein and 1.7 g lipid.

Durum wheat porridge. The results shown in the current paper were produced from further analyses of samples and data collected from the previously published study of wheat endosperm[27]. Milled macroparticles (denoted by median sizes of 0.11, 0.38, 1.01, 1.44 and 1.95 mm) of durum wheat endosperm (77 g) were combined with 150 ml of water and heated in a saucepan with vigorous stirring for 5 min at 85 °C, after which, 150 ml of cold water was added and heated for a further 5 min at 85 °C, then brought to the boiling point and kept at this temperature for a further 5 min. The resulting porridge was then removed from the heat source and rested at room temperature for 15 min before use in the DGM and SDM.

One cooked portion (~377 g) of durum wheat porridge contained 61.1 g potentially available carbohydrate (of which 60.0 g was starch and 0.5 g was total sugars), 4.5 g dietary fibre, 9.4 g protein and 1.5 g lipid.

DGM and SDM. For the oral phase, the cooked porridge, minus a 2-g weighed sub-sample (removed after cooking and used as a baseline), was mixed with 20 ml distilled water, then simulated salivary fluid (10 ml containing 0.15 M NaCl and 3 mM urea (pH 6.9)) and 1 ml human salivary α-amylase (900 U; Sigma–Aldrich; dissolved in simulated salivary fluid) were added. After 10 min, another 2-g sub-sample was collected to represent the effect of the simulated oral digestion phase.

For the gastric phase, the remaining mixture was added to the DGM, which was already primed with 20 ml acidified salt solution (58 mM NaCl, 30 mM KCl, 0.5 mM $CaCl_2$, 0.864 mM NaH_2PO_4 and 10 mM HCl), to simulate the contents of the stomach in fasted humans. Physiological additions of simulated gastric secretions containing 9,000 U ml^{-1} porcine gastric pepsin, 60 U ml^{-1} gastric lipase analogue from *Rhizopus oryzae* (Amano Enzyme) and 0.127 mM lecithin liposomes in an acidified salt solution occurred throughout gastric digestion. Gastric samples were ejected from the DGM every 10 min over a 60-min period.

For the duodenal phase, each gastric sample was immediately weighed, neutralized to pH 7.0 with 1 M NaOH and re-weighed. Next, 30 g of each neutralized gastric sample was transferred into individual bottles containing 3.75 ml of so-called hepatic mix and 11.25 ml of designated pancreatic mix, then placed on an orbital shaker (170 r.p.m.) at 37 °C to represent the duodenal digestion phase. The hepatic mix contained lecithin (6.5 mM; Lipid Products), cholesterol (4 mM), sodium taurocholate (12.5 mM) and sodium glycodeoxycholate (12.5 mM) in a salt solution of NaCl (146 mM), $CaCl_2$ (2.6 mM) and KCl (4.8 mM), and was prepared fresh for each run. The pancreatic mix contained pancreatic lipase (590 U ml^{-1}), porcine co-lipase (3.2 µg ml^{-1}), porcine trypsin (11 U ml^{-1}), bovine α-chymotrypsin (24 U ml^{-1}) and porcine α-amylase (300 U ml^{-1}) in a solution of NaCl (125 mM), $CaCl_2$ (0.6 mM), $MgCl_2$ (0.3 mM) and $ZnSO_4 \bullet 7H_2O$ (4.1 µM) and was prepared fresh for each run. A representative sub-sample (2 g) was removed at different time points (0.2, 2, 5, 10, 15, 20, 30, 40, 60, 90, 180 and 210 min) and added to ethanol (8 ml) for subsequent analysis of starch digestion products (total reducing sugars).

Overall, one cooked sample, one orally processed sample, six gastric samples and 72 (that is, 6 × 12) duodenal samples were collected per run. Two runs were performed with intact cells and one run was performed with freeze-milled samples. All analyses were performed in triplicate. Additional samples for microscopy analysis were collected at key time points, immediately immersed into Karnovsky's fixative and later processed and embedded in LR resin as described (see 'Light microscopy'). Samples for analysis of dry matter were frozen (−20 °C) in plastic pots and determined by oven drying at 102 °C.

Samples collected into ethanol for analysis of starch digestion were stored at 4 °C and centrifuged at 4,000*g* for 2 min before reducing sugar analysis. For the chickpea study, the reducing sugar concentration was determined by 3,5-dinitrosalicylic acid assay, as described elsewhere[10], whereas analysis of starch digestion products from durum wheat porridge was performed at Quadram Institute Bioscience (formerly the Institute of Food Research), as described previously[27]. The different reducing sugar assay methods used have been compared previously[28,29] and were selected based on the suitability of the working range and compatibility with samples obtained from these studies.

Data and statistical analysis. Graphing, curve fitting and statistical analyses were performed in GraphPad Prism (version 8.4.3; GraphPad software). Comparison of time-course data was performed by one-way analysis of variance, by mixed-effects model with Tukey's correction for multiple comparisons or by paired *t*-test, as indicated in the figure captions. Tukey's post-hoc test was applied when there was a significant effect of treatment. Statistically significant differences were accepted at $P < 0.05$. A paired *t*-test was used when only two curves were compared. Nonlinear regression analysis was applied to time-course data by least-squares regression to a one- or two-phase association equation, and 95% confidence intervals were obtained to show the probable location of the true curve.

Reporting Summary. Further information on research design is available in the Nature Research Reporting Summary linked to this article.

Data availability

Source data are provided with this paper. The other datasets generated and/or analysed during the current study are available from the corresponding author upon reasonable request.

Received: 19 December 2019; Accepted: 18 January 2021;
Published online: 18 February 2021

References

1. Stephen, A. M. et al. Dietary fibre in Europe: current state of knowledge on definitions, sources, recommendations, intakes and relationships to health. *Nutr. Res. Rev.* **30**, 149–190 (2017).
2. Grundy, M. M.-L. et al. Re-evaluation of the mechanisms of dietary fibre and implications for macronutrient bioaccessibility, digestion and postprandial metabolism. *Br. J. Nutr.* **116**, 816–833 (2016).
3. Jarvis, M. C., Briggs, S. P. H. & Knox, J. P. Intercellular adhesion and cell separation in plants. *Plant Cell Environ.* **26**, 977–989 (2003).
4. Golay, A. et al. Comparison of metabolic effects of white beans processed into 2 different physical forms. *Diabetes Care* **9**, 260–266 (1986).
5. Chu, J., Ho, P. & Orfila, C. Growth region impacts cell wall properties and hard-to-cook phenotype of canned navy beans (*Phaseolus vulgaris*). *Int. J. Food Process. Technol.* **13**, 818–826 (2020).
6. Pallares Pallares, A., Loosveldt, B., Karimi, S. N., Hendrickx, M. & Grauwet, T. Effect of process-induced common bean hardness on structural properties of in vivo generated boluses and consequences for in vitro starch digestion kinetics. *Br. J. Nutr.* **122**, 388–399 (2019).
7. Noah, L. et al. Digestion of carbohydrate from white beans (*Phaseolus vulgaris* L.) in healthy humans. *J. Nutr.* **128**, 977–985 (1998).
8. Petropoulou, K. et al. A natural mutation in *Pisum sativum* L. (pea) alters starch assembly and improves glucose homeostasis in humans. *Nature Food* **1**, 693–704 (2020).
9. Grassby, T. et al. Modelling of nutrient bioaccessibility in almond seeds based on the fracture properties of their cell walls. *Food Funct.* **5**, 3096–3106 (2014).
10. Edwards, C. H. et al. Manipulation of starch bioaccessibility in wheat endosperm to regulate starch digestion, postprandial glycemia, insulinemia, and gut hormone responses: a randomized controlled trial in healthy ileostomy participants. *Am. J. Clin. Nutr.* **102**, 791–800 (2015).
11. Würsch, P., Del Vedovo, S. & Koellreutter, B. Cell structure and starch nature as key determinants of the digestion rate of starch in legume. *Am. J. Clin. Nutr.* **43**, 25–29 (1986).
12. Dhital, S., Bhattarai, R. R., Gorham, J. & Gidley, M. J. Intactness of cell wall structure controls the in vitro digestion of starch in legumes. *Food Funct.* **7**, 1367–1379 (2016).
13. Rovalino-Córdova, A. M., Fogliano, V. & Capuano, E. The effect of cell wall encapsulation on macronutrients digestion: a case study in kidney beans. *Food Chem.* **286**, 557–566 (2019).
14. Edwards, C. H., Maillot, M., Parker, R. & Warren, F. J. A comparison of the kinetics of in vitro starch digestion in smooth and wrinkled peas by porcine pancreatic alpha-amylase. *Food Chem.* **244**, 386–393 (2018).
15. Edwards, C. H., Warren, F. J., Milligan, P. J., Butterworth, P. J. & Ellis, P. R. A novel method for classifying starch digestion by modelling the amylolysis of plant foods using first-order enzyme kinetic principles. *Food Funct.* **5**, 2751–2758 (2014).
16. Al-Rabadi, G. J. S., Gilbert, R. G. & Gidley, M. J. Effect of particle size on kinetics of starch digestion in milled barley and sorghum grains by porcine alpha-amylase. *J. Cereal Sci.* **50**, 198–204 (2009).
17. Korompokis, K., De Brier, N. & Delcour, J. A. Differences in endosperm cell wall integrity in wheat (*Triticum aestivum* L.) milling fractions impact on the way starch responds to gelatinization and pasting treatments and its subsequent enzymatic in vitro digestibility. *Food Funct.* **10**, 4674–4684 (2019).
18. Rovalino-Córdova, A. M., Fogliano, V. & Capuano, E. A closer look to cell structural barriers affecting starch digestibility in beans. *Carbohydr. Polym.* **181**, 994–1002 (2018).
19. Edwards, C. H. et al. A study of starch gelatinisation behaviour in hydrothermally-processed plant food tissues and implications for in vitro digestibility. *Food Funct.* **6**, 3634–3641 (2015).
20. Pitino, I. et al. Survival of *Lactobacillus rhamnosus* strains in the upper gastrointestinal tract. *Food Microbiol.* **27**, 1121–1127 (2010).
21. Vardakou, M. et al. Achieving antral grinding forces in biorelevant in vitro models: comparing the USP Dissolution Apparatus II and the Dynamic Gastric Model with human in vivo data. *AAPS PharmSciTech* **12**, 620–626 (2011).
22. Bhattarai, R. R., Dhital, S., Wu, P., Chen, X. D. & Gidley, M. J. Digestion of isolated legume cells in a stomach–duodenum model: three mechanisms limit starch and protein hydrolysis. *Food Funct.* **8**, 2573–2582 (2017).
23. Pallares Pallares, A. et al. Process-induced cell wall permeability modulates the in vitro starch digestion kinetics of common bean cotyledon cells. *Food Funct.* **9**, 6544–6554 (2018).
24. Wood, J. A. et al. Genetic and environmental factors contribute to variation in cell wall composition in mature desi chickpea (*Cicer arietinum* L.) cotyledons. *Plant Cell Environ.* **41**, 2195–2208 (2018).
25. Edwards, C. H., Cochetel, N., Setterfield, L., Perez-Moral, N. & Warren, F. J. A single-enzyme system for starch digestibility screening and its relevance to understanding and predicting the glycaemic index of food products. *Food Funct.* **10**, 4751–4760 (2019).
26. Goñi, I., Garcia-Alonso, A. & Saura-Calixto, F. A starch hydrolysis procedure to estimate glycemic index. *Nutr. Res.* **17**, 427–437 (1997).
27. Mandalari, G. et al. Durum wheat particle size affects starch and protein digestion in vitro. *Eur. J. Nutr.* **57**, 319–325 (2018).
28. Slaughter, S. L., Ellis, P. R., Jackson, E. C. & Butterworth, P. J. The effect of guar galactomannan and water availability during hydrothermal processing on the hydrolysis of starch catalysed by pancreatic alpha-amylase. *Biochim. Biophys. Acta* **1571**, 55–63 (2002).
29. Hussain, H., Ngaini, Z. & Chong, N. F.-M. Modified bicinchoninic acid assay for accurate determination of variable length reducing sugars in carbohydrates. *Int. Food Res. J.* **25**, 2614–2619 (2018).

Acknowledgements

We thank Premier Analytical Services (The Lord Rank Centre, High Wycombe, UK) for proximate analysis data on the wheat and chickpea samples, G. Campbell and S. Galindez-Najera (at the University of Manchester) for technical expertise, assistance and the use of facilities for preparation of the milled materials, G. Vizcay-Barrena from the Centre for Ultrastructural Imaging at King's College for sectioning microscopy samples, and the Model Gut team at the Institute of Food Research (now Quadram Institute Bioscience) for use of the DGM and SDM. This project was funded by the Biotechnology and Biological Sciences Research Council (BBSRC) (DRINC; BB/H004866/1) and C.H.E. was in receipt of a BBSRC CASE studentship award with Premier Foods (UK) as an industrial partner. C.H.E. gratefully acknowledges support from the BBSRC Institute Strategic Programme Food Innovation and Health (BB/R012512/1) and its constituent project (BBS/E/F/000PR10345).

Author contributions

C.H.E., P.R.E., G.M. and P.J.B. designed the research. C.H.E. conducted the research. C.H.E., P.R., G.M., P.R.E. and P.J.B. analysed the data. C.H.E. wrote the paper. P.R.E., P.R., G.M. and P.J.B. contributed to revisions of the manuscript. P.R.E. had primary responsibility for the final content. All of the authors read and approved the final manuscript.

Competing interests

The authors declare no competing interests.

Additional information

Supplementary information The online version contains supplementary material available at https://doi.org/10.1038/s43016-021-00230-y.

Correspondence and requests for materials should be addressed to C.H.E. or P.R.E.

Peer review information *Nature Food* thanks the anonymous reviewers for their contribution to the peer review of this work.

Reprints and permissions information is available at www.nature.com/reprints.

Publisher's note Springer Nature remains neutral with regard to jurisdictional claims in published maps and institutional affiliations.

nature research

Corresponding author(s): Peter R Ellis

Last updated by author(s): 16th January 2021

Reporting Summary

Nature Research wishes to improve the reproducibility of the work that we publish. This form provides structure for consistency and transparency in reporting. For further information on Nature Research policies, see Authors & Referees and the Editorial Policy Checklist.

Statistics

For all statistical analyses, confirm that the following items are present in the figure legend, table legend, main text, or Methods section.

n/a	Confirmed	
☐	☒	The exact sample size (*n*) for each experimental group/condition, given as a discrete number and unit of measurement
☐	☒	A statement on whether measurements were taken from distinct samples or whether the same sample was measured repeatedly
☐	☒	The statistical test(s) used AND whether they are one- or two-sided *Only common tests should be described solely by name; describe more complex techniques in the Methods section.*
☒	☐	A description of all covariates tested
☐	☒	A description of any assumptions or corrections, such as tests of normality and adjustment for multiple comparisons
☐	☒	A full description of the statistical parameters including central tendency (e.g. means) or other basic estimates (e.g. regression coefficient) AND variation (e.g. standard deviation) or associated estimates of uncertainty (e.g. confidence intervals)
☐	☒	For null hypothesis testing, the test statistic (e.g. *F*, *t*, *r*) with confidence intervals, effect sizes, degrees of freedom and *P* value noted *Give P values as exact values whenever suitable.*
☒	☐	For Bayesian analysis, information on the choice of priors and Markov chain Monte Carlo settings
☒	☐	For hierarchical and complex designs, identification of the appropriate level for tests and full reporting of outcomes
☒	☐	Estimates of effect sizes (e.g. Cohen's *d*, Pearson's *r*), indicating how they were calculated

Our web collection on statistics for biologists contains articles on many of the points above.

Software and code

Policy information about availability of computer code

Data collection	No software was used
Data analysis	GraphPad Prism (version 8.4.3, Graph Pad software, San Diago, CA, USA

For manuscripts utilizing custom algorithms or software that are central to the research but not yet described in published literature, software must be made available to editors/reviewers. We strongly encourage code deposition in a community repository (e.g. GitHub). See the Nature Research guidelines for submitting code & software for further information.

Data

Policy information about availability of data

All manuscripts must include a data availability statement. This statement should provide the following information, where applicable:

- Accession codes, unique identifiers, or web links for publicly available datasets
- A list of figures that have associated raw data
- A description of any restrictions on data availability

Source data for curves fitted in figure(s) 1, 3, 4 and 5 are provided with the paper, and the other datasets generated during and/or analysed during the current study are available from the corresponding author on reasonable request.

Field-specific reporting

Please select the one below that is the best fit for your research. If you are not sure, read the appropriate sections before making your selection.

☒ Life sciences ☐ Behavioural & social sciences ☐ Ecological, evolutionary & environmental sciences

Life sciences study design

All studies must disclose on these points even when the disclosure is negative.

Sample size	Sample size was based on prior studies. Study materials and conditions for lab experiments were well controlled and the number of samples used revealed large and reproducible differences between sample types./treatments.
Data exclusions	Data were not excluded from analysis.
Replication	Most experiments were performed three or more times with highly reproducible results (details of replication are provided in the manuscript). Greater variation between runs was observed in the Dynamic Gastric Model - this is taken into account in data interpretation.
Randomization	Not applicable as samples were not allocated to groups.
Blinding	Samples were coded during data collection, however true blinding could not be achieved in some studies due to the different physical appearance of the samples

Reporting for specific materials, systems and methods

We require information from authors about some types of materials, experimental systems and methods used in many studies. Here, indicate whether each material, system or method listed is relevant to your study. If you are not sure if a list item applies to your research, read the appropriate section before selecting a response.

Materials & experimental systems

n/a	Involved in the study
☒	☐ Antibodies
☒	☐ Eukaryotic cell lines
☒	☐ Palaeontology
☒	☐ Animals and other organisms
☒	☐ Human research participants
☒	☐ Clinical data

Methods

n/a	Involved in the study
☒	☐ ChIP-seq
☒	☐ Flow cytometry
☒	☐ MRI-based neuroimaging